The Influence of Monomer Structures on the Liquid Crystalline Order of Aramide Polymers: An NMR Analysis

Dan McElheny, Veronica Frydman, Min Zhou, and Lucio Frydman*

Department of Chemistry (M/C 111), University of Illinois at Chicago, 845 W. Taylor Street, Chicago, Illinois 60607-7061

Natural abundance NMR methods were employed to analyze the liquid crystalline behavior of poly(*p*-phenylene-2,6-naphthylamide) and poly(*p*-phenylene-4,4′-biphenylamide), two members of the aramide polymer family. These macromolecules were dissolved in absolute sulfuric acid and the extent of order in their liquid crystal phases was evaluated with the aid of solid phase ^{13}C tensor data and by total simulations of their lyotropic NMR line shapes as a function of temperature and concentration. These measurements revealed that as reported recently for other phenyl-based aramides, the nematic order of polymers in these lyotropic phases is essentially independent of temperature while slightly dependent on concentration. When considered in unison with these previous ^{13}C NMR analyzes this study also suggests that nematic order in aramides can be controlled by the choice of the monomeric chemical structures, increasing along the series naphthyl $\lesssim$ phenyl < biphenyl. Although the origin of this trend is not apparent when polymers are considered in their preferred all-anti/all-*trans* backbone conformations, its nature can be rationalized in terms of macromolecular semiflexibility arguments involving syn↔anti rearrangements of consecutive amide groups. These rearrangements impart worm-like displacements to otherwise rigid macromolecules that help understand the observed trend in order parameters, while simultaneously explaining the relative disorder exhibited by these aramide solutions in comparison with rigid rod theoretical predictions.

1. Introduction

The behavior of liquid crystalline polymers has made these macromolecules the focus of extensive theoretical and experimental investigations.[1−10] This interest has been further stimulated by the desirable material properties exhibited by these systems, which have propelled them during the last years into a wide variety of optical and mechanical applications.[11−13] The most characteristic feature of these macromolecules is their ability to organize into anisotropic fluid phases when molten or dissolved under appropriate conditions and then to retain these ordered arrangements upon being frozen or coagulated into solids. From the standpoint of molecular structure these polymers are usually classified as of main-chain or side-chain architecture, depending on whether the mesogenic groups promoting liquid crystallinity are positioned along the main polymer backbone or are pending from it via flexible spacers. Whereas side-chain polymers have been at the center of most nonlinear optics investigations structural applications have based almost exclusively on the main-chain arrangements. Among the most important members of this main-chain class are the aromatic polyamides (aramides), synthetic polymers which can be processed into fibers with very high tensile strength and superior chemical and thermal stabilities.[11,13−16]

Liquid crystallinity plays an important role in the processing of these aramides. When dissolved in absolute sulfuric acid at appropriate concentrations and temperatures these polymers form an anisotropic dope in which macromolecules are spontaneously ordered with respect to one another. These microscopic domains can be further aligned during industrial spinning under the effects of shearing flow fields, leading to macroscopically ordered fluids that are finally coagulated into bulk ordered

materials. This process highlights the relevance of understanding the mechanisms by which controllable factors, such as concentration, temperature, molecular weight, and monomeric structures, affect the anisotropic ordering in these fluid systems. Substantial progress has already been made in this area, both in terms of experimentally monitoring order parameters in aramide solutions[9,15,17−23] as well as in relating these order parameters to the statistical mechanics of the dissolved macromolecules.[2,6,10,24,25]

We have recently shown that natural abundance NMR techniques, particularly ^{13}C NMR data collected for the polymers in both their fluid and solid phases, can also be used as a quantitative tool for determining the dependencies of macromolecular order on different external and structural factors.[26,27] So far these analyses have focused on H_2SO_4 solutions of poly-(*p*-benzamide) (PBA, **1**), which can be considered as the parent compound of the aramide series, and of poly(*p*-phenylene-terephthalamide) (PPTA, **2**), the polymer that serves as basis for the Kevlar brand of commercial fibers. Molecular order in the anisotropic fluid phases of these polymers was found largely independent of temperature or molecular weight, while slightly dependent on polymer concentration. Except for this minor dependence the polymer order parameters that could be measured were remarkably similar—essentially identical—for both PBA and PPTA. This coincidence prompted the present study, whose main goal was to elucidate to what degree, if any, can monomeric structures control the nematic alignment of aramide polymers dissolved in H_2SO_4. By investigating this issue we expected to address practical details regarding the usefulness of searching for enhanced polymer alignment via chemical manipulations, as well as to yield further insight regarding the interplay between structure and liquid crystallinity in aramide
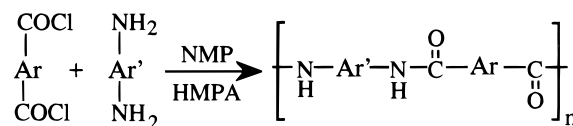
CHART 1

SCHEME 1
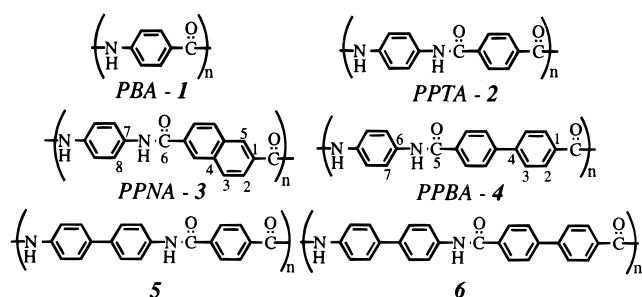
solutions. To achieve these goals a series of PPTA-derived analogs incorporating polynuclear aromatic moieties were synthesized (compounds **3**−**6**, Chart 1) and their mesogenic order explored using a combination of fluid and solid phase NMR techniques similar to those previously applied on PPTA and PBA. Unfortunately, only two of the synthesized polymers, poly(*p*-phenylene-2,6-naphthylamide) (PPNA, **3**) and poly(*p*-phenylene-4,4′-biphenylamide) (PPBA, **4**), could be successfully processed into anisotropic dopes. Overall the sulfuric acid solutions of these aramides displayed spectroscopic behaviors similar to those previously reported for PPTA and PBA, both in terms of their concentration and their temperature dependencies. Noticeable differences, however, arose on comparing the degrees of macromolecular order characterizing these polymers vis a vis PBA and PPTA, with alignment being smallest for solutions of the naphthyl derivative and largest for solutions of the biphenyl one. Although a relation between this ordering trend and molecular structure was not evident when regarding the aramide chains as possessing all amide bonds and aromatic rings in their most stable trans and anti conformations, structures and order parameters could be related when considering occasional anti↔syn rearrangements of consecutive amide groups. Indeed by endowing the otherwise linear main chains with worm-like fluctuations, these conformational changes could reduce the macromolecular order parameters from the value expected on the basis of rigid-rod statistical models to the set that is actually observed by NMR.

2. Experimental Section

All the determinations described in the present study were carried out on polymer samples synthesized in our laboratory following guidelines described in patented procedures.[28,29] The main features of these preparations are summarized in Scheme 1. The average inherent viscosities measured for the resulting **3**−**5** polymers in 96% H_2SO_4 were 1.27, 0.5, and 0.30 dL g^{-1} respectively; the viscosity of **6** could not be determined due to its intractability. Solutions of these samples were then readied for NMR analysis by dissolving various quantities of the synthetic polymers in (100.0 ± 0.3)% H_2SO_4, prepared in turn by mixing appropriate amounts of concentrated (96%) and fuming (10% SO_3) acid and checked by titration right before its use. The dissolution of the polymers was assisted by vigorous mechanical stirring of the suspensions during 48 h and performed inside an ice−water bath to prevent potential sample degradation. Concentrated solutions of **3** and **4** prepared in this manner were homogeneous, of a pale yellow color, and showed upon stirring the characteristic opalescence of lyotropic polymers. Polymer **5** on the other hand only led to dark isotropic solutions as apparently its molecular weight was not high enough for preventing degradation by the action of the concentrated acid. Compound **6** failed to yield anisotropic H_2SO_4 solutions or even isotropic ^{13}C NMR spectra with reasonable signal-to-

noise ratios, as this biphenyl-biphenyl aramide was intractable even in 10% free SO_3 fuming acid. Because of these reasons the main focus of the present work is on PPNA and PPBA and on their comparison with our previous PBA and PPTA determinations.

All NMR measurements were carried out at 7.1 Tesla using a two-channel laboratory-built NMR spectrometer. The fluid-phase measurements were performed on 5 mm samples employing a double-tuned Cryomagnetics probehead and a vertical spinning stack. ^{13}C spectra were collected using WALTZ-16 ^1H-decoupling, 100 ms acquisition times, no Overhauser enhancement, relatively long (≥2 s) relaxation delays to attempt spectral quantitativeness, an average of 3000 scans, and 9 μs π/2 excitation pulses. Thirty-two scans were usually collected in the ^1H solution acquisitions. Care was taken to achieve a reliable reading of temperatures, which were calibrated with an ethylene glycol standard and controlled using a laboratory-built variable temperature system. In order to analyze the liquid crystal polymer spectra and estimate macromolecular order parameters from their anisotropic shifts, solid phase measurements of the individual ^{13}C shielding tensor parameters were also carried out. These were performed using the 2D variable-angle correlation spectroscopy (VACSY) protocol, capable of separating undistorted powder patterns for chemically inequivalent sites by processing signals acquired as a function of different sample spinning angles with respect to the external magnetic field.[30] These data were acquired on a dynamic-angle-spinning probehead constructed around a 5 mm Doty stator and interfaced to a variable-angle motor and controller system governed by the Macintosh computer running the spectrometer. Such solid NMR experiments involved cross polarization, sample spinning at rates exceeding 6 kHz, and ^1H decoupling with 75 kHz rf fields. All chemical shifts in both the solid and solution experiments were referenced to $\delta_{TMS} = 0$ ppm using external references (adamantane and benzene respectively); they are estimated to be accurate to within ±0.3 ppm for the ^{13}C and ±0.1 ppm for the ^1H solution data.

3. Results

3.1. PPNA/H$_2$SO$_4$ NMR Spectra: Concentration and Temperature Dependence. Figure 1 illustrates the changes exhibited by the room temperature ^{13}C and ^1H NMR spectra of PPNA/H_2SO_4 solutions on changing the concentration of the dissolved polymer. At a 4% w/w polymer concentration the ^{13}C trace exhibits peaks that can be assigned simply on the basis of standard substituent chemical shift effects (Table 1). The ^1H NMR spectrum is entirely dominated by the H_2SO_4 resonance appearing at 11.0 ppm; no attempts were made to detect the much weaker solute peaks using solvent suppression techniques. As the polymer concentration increases a new set of peaks emerges in both the ^{13}C and ^1H traces, and these eventually become the sole spectral features at the highest concentrations. These changes are fully reversible and can be attributed to the formation of liquid crystalline domains where both solute and solvent molecules feel the effects of anisotropic chemical shift contributions, and hence, originate peaks that are shifted relative to their isotropic counterparts by amounts that depend on the polymer's degree of nematic order. The onset of this anisotropic
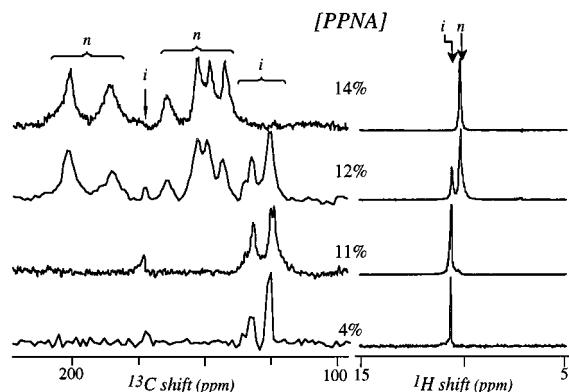
Liquid Crystalline Order of Aramide Polymers

J. Phys. Chem. B, Vol. 103, No. 44, 1999 **9507**

Figure 1. Concentration dependence of the room temperature ^{1}H and ^{13}C NMR spectra observed for PPNA/H$_2$SO$_4$ solutions. The letters "*i*" and "*n*" are used to denote the signals arising from the isotropic and nematic phases.

TABLE 1: Assignment of the ^{13}C NMR Resonances Observed in the Isotropic and Nematic Phases of PPBA and PPNA

	chemical shifts PPNA (in ppm)		chemical shifts PPBA (in ppm)	
site[a]	isotropic (expected)[b]	nematic[c]	isotropic (expected)[b]	nematic[c]
1	133.0 (134)	185	134.0 (133)	214
2	125.4 (126)	152	129.5 (128)	161
3	133.0 (131)	152	128.8 (127)	157
4	135.0 (134)	164	146.7 (143)	223
5	126.4 (130)	144	172.3 (168)	204
6	172.4 (168)	201	133.2 (134)	194
7	136.0 (134)	201	125.4 (119)	158
8	125.4 (119)	148		

[a] Numbered as shown in Chart 1. [b] Based on shifts calculated for NH$_2$CO-naphthyl-CONH$_2$, NH$_2$CO-biphenyl-CONH$_2$ derivatives. [c] Based on analyses of the nematic spectra (see text).
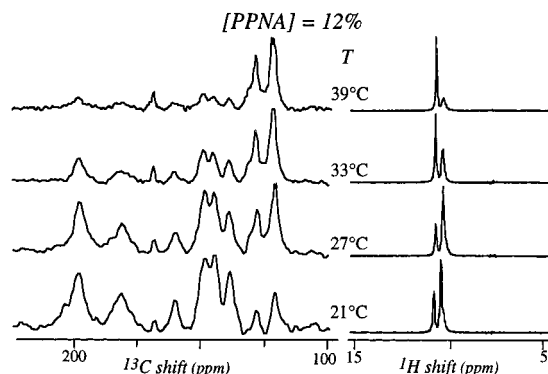

Figure 2. Temperature dependence shown by the ^{13}C and ^{1}H NMR spectra of 12% w/w PPNA/H$_2$SO$_4$ solutions.

phase should also result in proton-proton dipolar splittings, apparently absent from the ^{1}H NMR spectra of the solvent most likely as a result of fast intermolecular proton migrations within the H$_2$SO$_4$. These anisotropic displacements also lift many of the accidental degeneracies that characterize the otherwise poorly resolved isotropic ^{13}C spectrum of PPNA/H$_2$SO$_4$; their analysis is further discussed below.

Overall, the changes observed in these ^{1}H and ^{13}C NMR spectra are qualitatively similar to those that we have observed in earlier studies of PPTA and PBA solutions. As was also the case in those systems noticeable changes are displayed by both ^{13}C and ^{1}H NMR if polymer concentrations are kept constant but the temperature is changed (Figure 2). These changes affect the relative intensities of isotropic and anisotropic resonances in the region of biphasic coexistence and are fully reversible
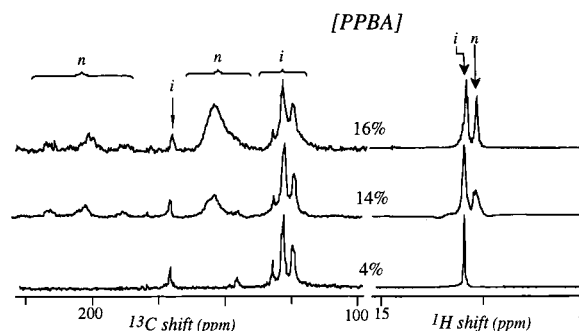

Figure 3. Concentration dependence of the room temperature PPBA/H$_2$SO$_4$ NMR spectra.
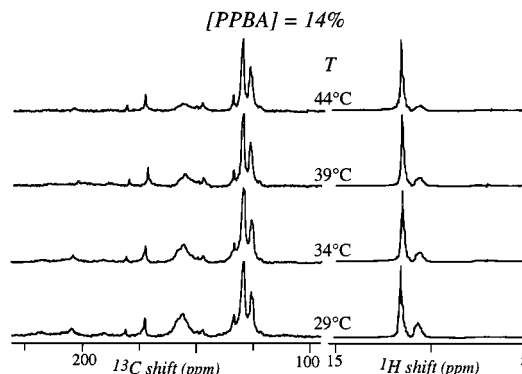

Figure 4. Temperature dependence of a 14% w/w PPBA/H$_2$SO$_4$ solution.

up to temperatures of about 50 °C; beyond this point the polymer apparently begins to decompose in the concentrated acid environment, leading to smaller fragments that are less prone to form anisotropic arrangements and thus enhance the intensities of the isotropic signals. Another characteristic of these lyotropic spectra is that the anisotropic ^{13}C resonances do not shift, at least within our experimental accuracy, when studied as a function of temperature; they do however vary slightly (~1 ppm on average at 27 °C) upon changing the polymer's concentration from 12 to 14%.

3.2. PPBA/H$_2$SO$_4$ NMR: Concentration and Temperature Dependence. The general features displayed by the acid solutions of PPNA are also found in the case of PPBA/H$_2$SO$_4$. When dilute, PPBA yields conventional ^{13}C NMR spectra with seven distinct peaks (Figure 3) whose assignments can be tentatively carried out on the basis of substituent chemical shift effects (Table 1). As its concentration increases, a new set of downfield peaks emerges whose origin can again be explained by the appearance of anisotropic polymer domains. The changes characterizing the ^{1}H NMR spectra of these solutions are similar to those shown by the other aramides except for the fact that even at the relatively high concentration of 16% w/w the fluid is still an approximately 1:1 biphasic mixture, probably a reflection of PPBAs generally lower molecular weight. The ^{13}C NMR spectrum of nematic PPBA is also quantitatively different from those displayed by other liquid crystalline aramides, in that some of its resonances are shifted further downfield than in any of the other samples we have investigated. On the other hand, the temperature dependence that NMR reveals for the phase equilibrium of PPBA/H$_2$SO$_4$ solutions is similar to the one exhibited by the other aramides, with a decrease in the fraction of the nematic phase with temperature (Figure 4) and no apparent temperature dependence in the absolute positions of the nematic resonances.

For both PPNA/H$_2$SO$_4$ and PPBA/H$_2$SO$_4$ the changes in relative peak intensities with temperature can be viewed as
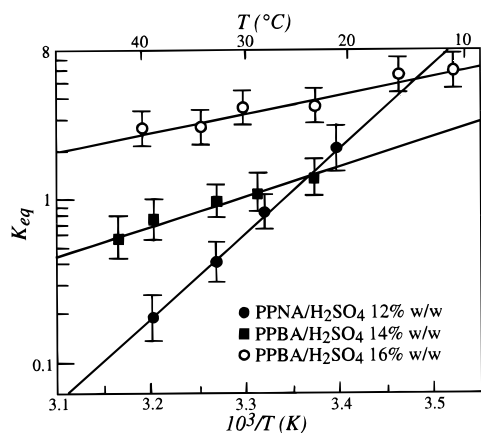
Figure 5. Van't Hoff diagrams resulting from plotting the ratios between peaks arising from the liquid crystalline and isotropic phases as a function of inverse temperature. Lines indicate the best fit of the data and lead to the parameters listed in Table 2.

TABLE 2: Thermodynamic Parameters Characterizing Isotropic ⇌ Nematic Equilibria in Various Aramide Solutions

system	ΔH (kcal mol^{-1})	ΔS (cal K^{-1} mol^{-1})
PBA, 11% w/w[a]	-16 ± 1	-57 ± 6
PBA, 12.4% w/w[a]	-20 ± 2	-63 ± 7
PPTA, 12% w/w[b]	-17 ± 1	-47 ± 5
PPNA, 12% w/w[c]	-27 ± 4	-90 ± 10
PPBA, 14% w/w[c]	-11 ± 2	-37 ± 5
PPBA, 16% w/w[c]	-8 ± 2	-30 ± 5

[a] From ref 27. [b] From ref 26. [c] This study.

reflecting a phase equilibrium

Polymer (isotropic phase) ⇌

Polymer (liquid crystalline phase),

for which both the ^{13}C and ^{1}H NMR peaks can provide an effective equilibrium constant K_{eq} in terms of the ratios between peaks originated in each phase. These in turn can lead to Van't Hoff plots describing the enthalpic and entropic characteristics of the dynamic equilibria for the different solutions (Figure 5). A comparison between these thermodynamic parameters and those previously reported for various PBA and PPTA solutions in sulfuric acid is summarized in Table 2; interesting systematic differences can be observed in these parameters among the various polymers, although their assessment at this point is complicated by the different molecular weights of the analyzed samples.

3.3. Quantitative Description of the [13]C Nematic Spectra. As known from the liquid crystalline NMR literature ^{13}C NMR data can be employed to quantify the anisotropic characteristics of lyotropic solutions such as those originated by aramides in H_2SO_4.[31] Indeed the degree of order attained by the various polymer chemical sites in the nematic phase can be characterized by the ^{13}C shifts $\Delta\delta$ occurring when macromolecules cease to tumble isotropically and become aligned with respect to a macroscopic director:

$$\Delta\delta = \delta_{\text{aniso}} - \delta_{\text{iso}} \tag{1}$$

These site specific ^{13}C NMR displacements can in turn be related to the local ordering matrix $\{S_{ij}\}_{i,j=1,2,3}$ according to

$$\Delta\delta = \frac{2}{3}\sum_{i,j=1,2,3} S_{ij}\delta_{ij} \tag{2}$$

where $\{1,2,3\}$ represents the orientation of an arbitrary orthogonal axis system and $\{d_{ij}\}_{i,j=1,2,3}$ represent the elements that within the same axis system describe the anisotropy of the site's chemical shift tensor. For the case of strongly anisometric and uniaxial lyotropics like those represented by aramide polymers the order description can be cast in terms of a single order parameter S_{zz} that describes the average orientational order of the macromolecular chains with respect to their overall macroscopic director. Equation 2 can then be rewritten as

$$\Delta\delta = \frac{2}{3}S_{zz}\delta_{zz} \tag{3}$$

where δ_{zz} represents now the effective anisotropic shielding component of a particular site along the director's axis, once the averaging effects caused by all possible intramolecular motions have been taken into account. It follows from these considerations that ^{13}C NMR can be used to quantify the degree of anisotropic order in these various lyotropic solutions, provided that the chemical shift displacements $\Delta\delta$ undergone by each site upon going from the isotropic to the liquid crystalline phase is determined and that the local anisotropic parameters δ_{zz} of these sites are individually measured.

Establishing the $\Delta\delta$ displacements requires correlating each anisotropic peak with its isotropic counterpart, a task that for simple systems can be carried out on the basis of "educated guesses" and which for more complex spectra can benefit from spectroscopic techniques such as variable-angle sample spinning[32] or the recently developed dynamic director NMR approach.[33] The application of this spectroscopic method to the elucidation of isotropic and anisotropic ^{13}C chemical shifts in liquid crystalline and aramide spectra will be further exemplified in a future contribution; for the sake of the present analysis we summarize the necessary results with the assignments of the various ^{13}C peaks in the two phases (Table 1).

The remaining parameters involved in the analysis, the various δ_{zz}, were computed for each atomic site in the polymers with the aid of solid state ^{13}C NMR measurements capable of yielding the full shift anisotropy of the individual sites. These were intended to be two-dimensional variable-angle correlation spectroscopy (VACSY) NMR runs on the solid polymers, as this experiment can separate each site's characteristic powder NMR spectrum according to its isotropic ^{13}C chemical shift. Unfortunately, even with the MAS-like spectral resolution of this procedure and with the aid of spectral editing methods, the large number of chemically similar aromatic carbons and the line broadening typical of these heterogeneous polymers prevented the full resolution and characterization of all solid state NMR resonances in PPNA and PPBA. Because of this reason, the tensor elements of the various carbon sites in the polymer had to be estimated from NMR measurements on simpler, model compounds. The specific strategy adopted was therefore the following: for the two inequivalent sites in the diaminophenyl units of both PPNA and PPBA ($-NH-C_6H_4-NH-$), it was assumed that the shielding anisotropy parameters were equal to those recently measured by VACSY for the similar moiety in PPTA.[34] The ^{13}C shielding tensors for the polynuclear ring of PPBA were then estimated from the values measured in the synthetic precursor biphenyldicarboxyl chloride, for which a conventional 2D cross polarization VACSY acquisition could resolve all but two of the chemically inequivalent sites (Figure 6); the parameters for these two overlapping sites were assumed equal. For the naphthyl ring of PPNA the ^{13}C tensor values were also estimated from 2D VACSY NMR experiments on the naphthyldicarboxyl chloride precursor, for which short contact

Liquid Crystalline Order of Aramide Polymers
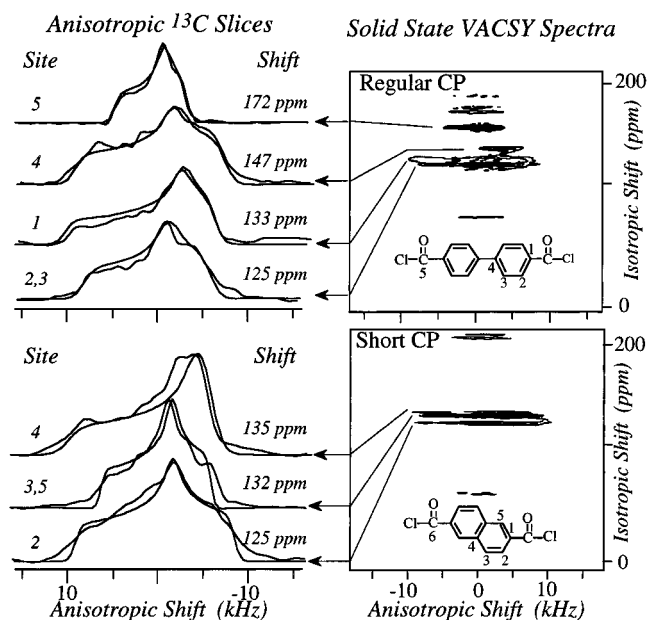
J. Phys. Chem. B, Vol. 103, No. 44, 1999 **9509**

Figure 6. Summary of the solid state NMR VACSY data acquired for estimating the chemical shift tensor parameters of the various chemical sites in PPNA, PPBA. The 2D ^{13}C NMR spectra of the indicated precursors are shown as contour plots; the individual ^{13}C powder line shapes extracted from them are shown superimposed on top of their best fit simulations.

TABLE 3: ^{13}C Chemical Shift Tensor Elements Used in the Analyses of PPNAs and PPBAs Lyotropic Spectra[a]

	elements PPNA (in ppm)				elements PPBA (in ppm)		
site[b]	δ_{11}	δ_{22}	δ_{33}	site[b]	δ_{11}	δ_{22}	δ_{33}
1[c]	245	122	31	1[d]	245	122	31
2[d]	248	145	−18	2[d]	226	154	10
3[d]	223	148	28	3[d]	224	152	8
4[d]	205	205	−5	4[d]	235	152	7
5[d]	216	141	21	5[e]	226	188	102
6[e]	258	165	95	6[c]	230	155	14
7[c]	233	158	17	7[c]	211	151	13
8[c]	211	151	13				

[a] Isotropic solid phase shifts accurate within ±1 ppm; individual tensor elements accurate within ±5 ppm. [b] As labeled in Chart 1. [c] Tensor elements measured on PPTA (ref 34). [d] Tensor elements taken from the acyl chloride precursors. [e] Tensor elements measured in the polymers themselves.

times (70 μs) resolved the protonated site 2 from the superimposed resonances of sites 3 and 5; the anisotropies of these overlapping sites were again assumed equal. Fortuitously, this VACSY experiment also showed a weak but discernible signal from the bridgehead site 4 whose anisotropy was thus also incorporated into the analysis; this site's values resulted remarkably close to those reported for the bridgehead site in a single crystal of naphthalene.[35] Finally, the shielding tensors of the carbonyl amide sites could be clearly observed in 2D VACSY acquisitions of the polymer samples themselves; a summary of all these solid state chemical shift anisotropy parameters is presented in Table 3.

With the principal elements $\{\delta_{ii}\}_{i=1-3}$ describing the sites' chemical shielding tensors known the effective anisotropic chemical shift displacements could be calculated as

$$\delta_{zz} = \sum_{l=-2}^{2} \langle \mathcal{D}_{l,0}^{(2)}(\Omega) \rho_{2,l} \rangle \qquad (4)$$

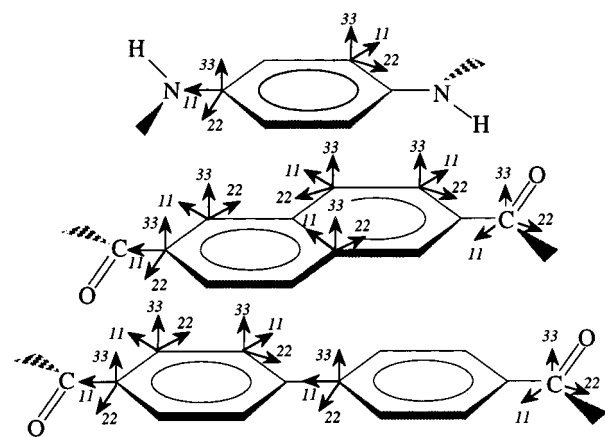where the brackets indicate that rapid averaging motions

Figure 7. Orientations assumed for the principal axes systems of the various ^{13}C sites in PPNA and PPBA. The individual $(ii)_{i=1-3}$ labels correspond to the various $(\delta_{ii})_{i=1-3}$ components summarized in Table 3; the angles between the carbonyls δ_{11} axes and the C−C bonds were assumed 40° for both naphthyl and biphenyl groups.
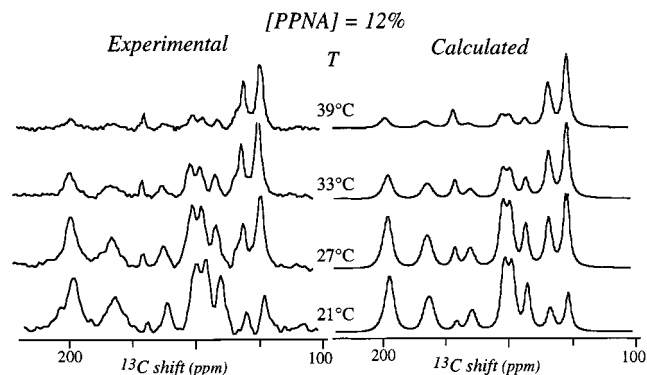

Figure 8. Comparison between the experimental ^{13}C NMR spectra arising from a 12% w/w PPNA/H$_2$SO$_4$ solution (left), and best fit simulations calculated as described in the text. These total line shape simulations assumed temperature dependent fractions of the isotropic and nematic phases (Figure 5), constant order parameters (Table 4), and peak intensities in proportion to the abundance of each site in the monomer.
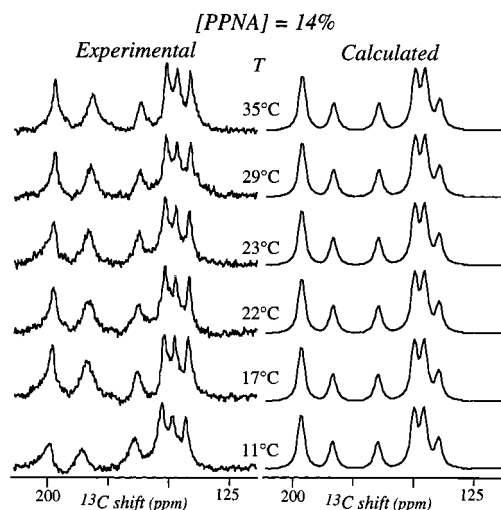

Figure 9. Same as that in Figure 8 but for a 14% w/w PPNA solution; no isotropic peaks appear under these conditions regardless of temperature.

executed by the polymer chains in the liquid crystal have been considered, the spherical tensor elements $\{\rho_{2,l}\}_{-2 \le l \le 2}$ are defined as $\rho_{2,0} = \sqrt{3/2}(\delta_{33} - \delta_{iso})$, $\rho_{2,\pm 1} = 0$ and $\rho_{2,\pm 2} = (\delta_{22} - \delta_{11})/2$,
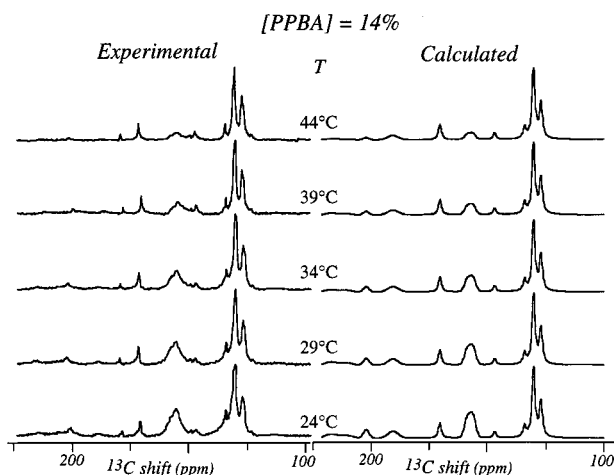
Figure 10. Same as that in Figure 8 but for a 14% w/w PPBA/H$_2$SO$_4$ solution.
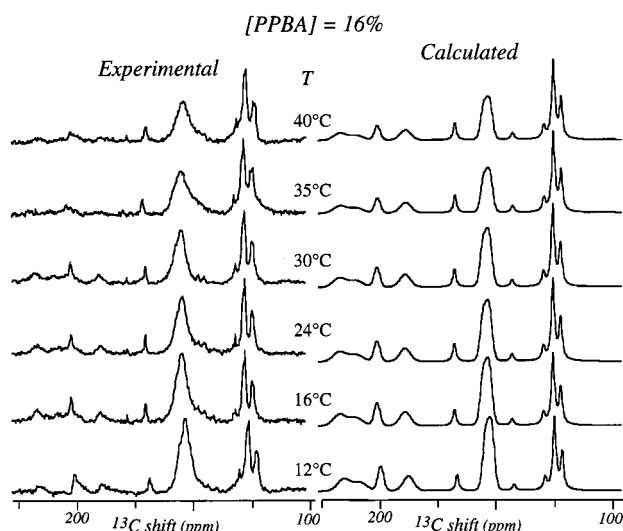

Figure 11. Same as that in Figure 10 but for a 16% w/w concentration.

and the Wigner rotational matrices $\{\mathcal{D}_{l,0}^{(2)}(\Omega)\}_{-2\leq l\leq 2}$ relate the orientations of these tensors with the nematic director axis.[36] In order to evaluate eq 4, it was assumed that the only two dynamic processes averaging the δ_{zz} values were fast rotations of the aromatic groups about their axial substituents, and fast rotations of the polymer chains about their main axes. The (α,β,γ) angles orienting each site shielding tensor with respect to the first of these averaging axes were taken from literature guidelines (Figure 7);[37] the angles between the *para* axes of these aromatic groups and the main polymer chain axes were then extracted with the aid of molecular modeling calculations (10°, 12°, and 16° for the biphenyl, phenyl, and naphthyl groups respectively).

With all these NMR coupling parameters defined, the order and phase behaviors of PPNA/H$_2$SO$_4$ and PPBA/H$_2$SO$_4$ solu-

TABLE 4: Lyotropic Order Parameters Afforded by the ^{13}C NMR Analyses of Different Aramide/H$_2$SO$_4$ Solutions

system	order parameter ($\pm 0.01^a$)
PPNA 12% w/w[b]	0.62
PPNA 14% w/w[b]	0.64
PPTA 12% w/w[c]	0.66
PBA 12.4% w/w[d]	0.67
PBA 14% w/w[d]	0.70
PPBA 14% w/w[b]	0.78
PPBA 16% w/w[b]	0.79

[a] Error margins resulting from direct visual comparisons between experiments and fits, assuming that data in Figure 7 and Table 3 accurately reflect the coupling parameters of PPNA and PPBA. [b] From Figures 8−11. [c] From ref 26. [d] From ref 27.

tions as a function of concentration and temperature could be successfully quantified. Figures 8−11 summarize these analyses by comparing various sets of experimental ^{13}C NMR spectra with their best fit total line shape simulations. For each experimental spectrum these calculations involved adjusting three independent fitting parameters: the relative fraction of coexisting isotropic/nematic phases (K_{eq} in Figure 5), the order parameter of macromolecules in the nematic phase (S_{zz} in eq 3), and the broadening of the spectral lines. All these parameters have very distinctive effects on the outcome of the simulations and are therefore highly uncorrelated; in all cases the agreement observed between the calculated and experimental traces was very good.

4. Discussion and Conclusions

As mentioned in the Introduction one of the main goals of this study was to elucidate what roles could monomeric structures play in determining the degree of alignment adopted by aramide polymers in lyotropic H$_2$SO$_4$ solutions. Table 4 compares the order parameters measured previously for PBA and PPTA with those measured now for the various PPNA and PPBA solutions. It follows from this table that the order parameters measured previously for PPTA and PBA solutions were fortuitously identical, because macromolecular order in these aramide/H$_2$SO$_4$ solutions follows the trend

$$S_{zz}^{PPNA} \lesssim S_{zz}^{PPTA} \approx S_{zz}^{PBA} < S_{zz}^{PPBA} \qquad (5)$$

This trend is constant with temperature, largely independent of concentration, and it does not correlate with the molecular weight of the various polymers (which, at least judging from inherent viscosities, was highest for the PPNA and lowest for the PPBA sample). It is therefore reasonable to assume that it is reflecting the interplay between the differing monomeric structures and the macromolecular order in this type of systems.

A cursory look at the ideal structures of the analyzed aramides does not necessarily clarify the mechanism that originates the ordering behavior summarized in eq 5: dicarbonylic aromatic
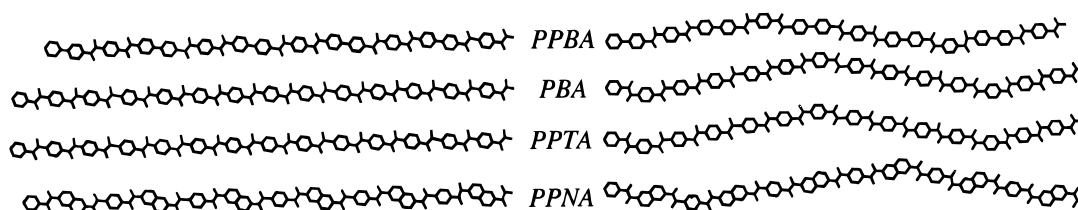

Figure 12. Different potential geometries adopted by aramide polymers in their lyotropic solutions. When aramide groups are in their preferred anti conformations all chains are equally linear (left), but occasional syn arrangements of consecutive amide groups introduce a semiflexibility that can potentially link rigid rod liquid crystal models with the NMR observations (right).

Liquid Crystalline Order of Aramide Polymers

J. Phys. Chem. B, Vol. 103, No. 44, 1999 **9511**

rings arranged in their preferred anti substitution patterns and possessing their amide groups in ideal trans conformations can be expected to yield equally linear aramide chains regardless of whether they involve naphthyl, phenyl or biphenyl rings (Figure 12, left). Deviations from this ideal linear-rod conformations are therefore needed to account for the varying degrees of order revealed by NMR. One such possible source of non-ideality could reside in a departure of the amide groups from their ideal sp^2 geometries;[38] molecular models, however, fail to predict that bond angles other than 120° will be substantially more or less likely for any one of the analyzed derivatives. Cis conformations of the amide groups could also disrupt substantially the polymer linearity and lead to the occurrence of hairpins defects; again, however, no link is evident between the appearance of these sharp defects and the various monomeric structure. Another mechanism capable of disturbing the linearity of the polymer chains is the appearance of occasional syn configurations for consecutive amide groups, a rearrangement that should be energetically less demanding than the other two and therefore perhaps more likely. Simple models reveal that this mechanism would lead to structure-dependent distortions that correlate well with the trends observed by NMR. Indeed the chain deflections resulting from random anti↔syn rearrangements of consecutive amide groups are the smallest for the case of PPBA, almost identical for the phenyl-based PBA and PPTA and slightly larger than these for the naphthyl polymer (Figure 12, right). The semiflexibility provided by this degree of conformational freedom could also help explain why the order parameters observed by ^{13}C NMR for these aramide polymers are consistently smaller than the minimum order parameter predicted by statistical models for solutions of ideal rigid rods ($S_{zz} > 0.79$).[39] In fact it can be naively estimated that an average of ≈1.8 syn conformations per polymer chain would scale down this ideal rigid-rod solution order parameter to within 4% of all the order parameter values experimentally observed for the analyzed aramides. Because of the crudeness of this model it is conceivable that such numerical agreement is mostly coincidental; yet, it is mentioned because of the support it lends to such line of reasoning. The quantitativeness of this analysis is also compromised by the possibility of "crankshaft" motions that could partially compensate for this form of aramide semiflexibility without affecting the order parameters[40] and by the inability of NMR to detect any of the chemically inequivalent ^{13}C sites associated to the minority *syn* conformation. Such objections, however, could be accounted for by a more sophisticated model in which syn defects effectively displace throughout the chain bringing about pseudorotations of the aromatic groups, while dynamically averaging away inequivalencies among the NMR resonances. Further evaluations of these observations and models could therefore benefit from more detailed NMR studies on the nature of segmental distributions in lyotropic aramides, as well as from analyses on the dependencies of these distributions on physical and chemical factors; such studies are currently under way.

References and Notes

(1) Blumstein, A., Ed. *Liquid Crystalline Order in Polymers*; Academic Press: New York, 1978.
(2) Ciferri, A., Krigbaum, W. R., Meyer, R. B., Eds. *Polymer Liquid Crystals*; Academic Press: New York, 1982.
(3) Samulski, E. T. *Phys. Today* **1982**, *35*, 40.
(4) Gordon, M., Cantou, H.-J., Eds. *Liquid Crystal Polymers*. In *Advances in Polymer Science*; Springer: Berlin, 1984; Vols. 59−61.
(5) Chapoy, L. L., Ed. *Recent Advances in Liquid Crystalline Polymers*; Elsevier: Amsterdam, 1985.
(6) Odijk, T. *Macromolecules* **1986**, *19*, 2313.
(7) Finkelmann, H. *Angew. Chem., Int. Ed. Engl.* **1987**, *26*, 816.
(8) Tsvetkov, V. N. *Rigid Chain Polymers*; Plenum: New York, 1989.
(9) Northolt, M. G.; Sikkema, D. J. *Adv. Polym. Sci.* **1990**, *98*, 115.
(10) Sato, T.; Teramoto, A. *Adv. Polym. Sci.* **1996**, *126*, 85.
(11) Yang, H. H. *Aromatic High-Strength Fibers*; Wiley: New York, 1989.
(12) *Liquid Crystalline Polymers*; Carfagna, C., Ed.; Pergamon Press: Oxford, 1994.
(13) *Liquid Crystalline Polymer Systems*; Isayev, A. I., Kyu, T., Cheng, S. Z. D., Eds.; American Chemical Society: Washington, 1996.
(14) Bair, T. I.; Morgan, P. W.; Killian, F. L. *Macromolecules* **1977**, *10*, 1396.
(15) Kwolek, S. L.; Morgan, P. W.; Schaefgen, J. R.; Gulrich, L. W. *Macromolecules* **1977**, *10*, 1390.
(16) Ciferri, A. In *Developments in Oriented Polymers*; Ward, I. M., Ed.; Elsevier: London, 1987; Vol. 2, Chapter 3.
(17) Fan, S. M.; Luckhurst, G. R.; Picken, S. J. *J. Chem. Phys.* **1994**, *101*, 3255.
(18) Picken, S. J. *Macromolecules* **1989**, *22*, 1766.
(19) Lin, J.; Li, S. *Eur. Polym. J.* **1994**, *30*, 671.
(20) Papkov, S. P.; Kulichikhin, V. G.; Kalmikova, V. G.; Malkin, A. Y. *J. Polym. Sci., Polym. Phys. Ed.* **1974**, *12*, 1753.
(21) Balbi, C.; Bianchi, E.; Ciferri, A.; Tealdi, A.; Krigbaum, W. R. *J. Polym. Sci., Polym. Phys. Ed.* **1980**, *1980*, 2037.
(22) Sartirana, M. L.; Marsano, E.; Bianchi, E.; Ciferri, A. *Macromolecules* **1986**, *19*, 1176.
(23) Papkov, S. P.; Iovleva, M. M.; Ivanova, N. A.; Andreyeva, I. N.; Kalmykova, V. D.; Volokhina, A. V. *Polym. Sci. USSR* **1979**, *20*, 742.
(24) Flory, P. J.; Ronca, G. *Mol. Cryst. Liq. Cryst.* **1979**, *59*, 311.
(25) Flory, P. J. *Adv. Polym. Sci.* **1984**, *59*, 1.
(26) Zhou, M.; Frydman, V.; Frydman, L. *J. Phys. Chem.* **1996**, *100*, 19280.
(27) Zhou, M.; Frydman, V.; Frydman, L. *Macromolecules* **1997**, *30*, 5416.
(28) Kwolek, S. L. U.S. Patent 3,671,542; June 20, 1972.
(29) Kwolek, S. L. U.S. Patent 3,819,582; June 25, 1974.
(30) Frydman, L.; Chingas, G. C.; Lee, Y. K.; Grandinetti, P. J.; Eastman, M. A.; Barrall, G. A.; Pines, A. *J. Chem. Phys* **1992**, *97*, 4800.
(31) Emsley, J. W. In *NMR of Liquid Crystals*; Emsley, J. W., Ed.; Reidel Publishers: Dordrecht, 1985, pp 379 and ff.
(32) Courtieu, J.; Bayle, J. P.; Fung, B. M. *Prog. NMR Spectrosc.* **1994**, *26*, 141.
(33) Zhou, M.; Frydman, V.; Frydman, L. *J. Am. Chem. Soc.* **1998**, *120*, 2178.
(34) Sachleben, J. R.; Frydman, L. *Solid State NMR* **1997**, *7*, 301.
(35) Sherwood, M. H.; Facelli, J. C.; Alderman, D. W.; Grant, D. M. *J. Am. Chem. Soc.* **1991**, *113*, 750.
(36) Haeberlen, U. *Advances in Magnetic Resonance*; Academic Press: New York, 1976.
(37) Facelli, J. C.; Grant, D. M. In *Topics in Stereochemistry*; Eliel, E. C., Willen, S. H., Eds.; Wiley: New York, 1989, pp 1 and ff.
(38) Tsvetkov, V. N.; Rjumtsev, E. I.; Shtennikova, I. N. In *Liquid Crystalline Order in Polymers*; Blumstein, A., Ed.; Academic Press, New York, 1978; Chapter 2.
(39) Lee, S.-D.; Meyer, R. B. *J. Chem. Phys.* **1986**, *84*, 3443.
(40) Papkov, S. P. *Adv. Polym. Sci.* **1984**, *59*, 75.